



HAL
open science

Plane wave propagation and normal transmission and reflection at discontinuity surfaces in second gradient 3D Continua

Francesco Dell'Isola, Angela Madeo, Luca Placidi

► **To cite this version:**

Francesco Dell'Isola, Angela Madeo, Luca Placidi. Plane wave propagation and normal transmission and reflection at discontinuity surfaces in second gradient 3D Continua. 2010. hal-00524991

HAL Id: hal-00524991

<https://hal.science/hal-00524991>

Preprint submitted on 10 Oct 2010

HAL is a multi-disciplinary open access archive for the deposit and dissemination of scientific research documents, whether they are published or not. The documents may come from teaching and research institutions in France or abroad, or from public or private research centers.

L'archive ouverte pluridisciplinaire **HAL**, est destinée au dépôt et à la diffusion de documents scientifiques de niveau recherche, publiés ou non, émanant des établissements d'enseignement et de recherche français ou étrangers, des laboratoires publics ou privés.

Plane wave propagation and normal transmission and reflection at discontinuity surfaces in second gradient 3D Continua

Francesco dell'Isola^{1,3}, Angela Madeo² and Luca Placidi^{3,4}

October 10, 2010

1 Dipartimento di Ingegneria Strutturale e Geotecnica, Università di Roma La Sapienza, Via Eudossiana 18, 00184, Roma, Italy

2 Laboratoire de Génie Civil et Ingénierie Environnementale, Université de Lyon–INSA, Bâtiment Coulomb, 69621 Villeurbanne Cedex, France

3 Laboratorio Strutture e Materiali Intelligenti, Fondazione Tullio Levi-Civita, Via S. Pasquale snc, Cisterna di Latina, Italy

4 DIS, Università Roma Tre, Via C. Segre 4/6, 00146 Roma, Italy

Abstract

We study propagation of plane waves in second gradient solids and their reflection and transmission at plane displacement discontinuity surfaces where many boundary layer phenomena may occur. Second gradient elastic moduli determine how planar waves behave at discontinuity surfaces. We explicitly remark that reflection and transmission coefficients which we have estimated show also a significant dependence on frequency: therefore the novel results presented can be the basis of experimental procedures to estimate some among these moduli.

1 Introduction

In Germain (1973a) and Germain (1973b) a consistent continuum theory allowing for the dependence of deformation energy on second gradient of placement is presented. The approach used in the aforementioned papers is based on the principle of virtual works. Let B be the body the motion of which needs to be described and let S be a regular sub-body of B : Germain, following the ideas already presented in Cosserat & Cosserat (1909), assumes that the external powers balance the internal powers plus inertial powers for every S . When there exists a deformation energy then the internal power can be represented as its first variation. When the system is conservative, the postulated principle of virtual works reduces to the assumption that the action functional is stationary.

On the other hand, it is possible, by means of a Hamilton-Rayleigh principle (see e.g. dell’Isola *et al.* (2009a)), to deduce a particular form of the principle of virtual works from given action and Rayleigh dissipation functionals. Germain’s theory does not fit Cauchy format for continuum mechanics. Indeed, so-called Cauchy postulate is seen to hold, actually, only for a class of materials which results to be rather particular. Indeed, it results that Cauchy postulate is actually a restriction on the set of constitutive equations which one is allowed to use. As already found at least by Casal (1961), when deformation energy depends on second gradient of displacement then contact surface force densities at every Cauchy cut must, in general, depend on the curvature of such Cauchy cut. Only in very particular cases (see e.g. dell’Isola & Seppecher (1997)) second gradient continua show contact actions of the type described by Cauchy. Germain’s main result reduces to stating that by means of the only Cauchy stress tensor one cannot describe the more complex contact interactions occurring in second gradient continua. Contact surface force densities depending on curvature of Cauchy cuts must arise in conjunction with i) contact double-force surface densities and ii) contact edge line force densities. Double-forces expend power on normal velocity gradients through Cauchy cuts and contact edge line density forces arise at those lines on Cauchy cuts where the normal suffers concentrated discontinuities. This point is thoroughly investigated in the literature: for more details we refer e.g. to dell’Isola & Seppecher (1995), dell’Isola & Seppecher (1997), dell’Isola & Seppecher (2010) and the references there cited. The structure of contact interactions in second gradient continua is much more complicated than in the case of Cauchy continua and needs a more sophisticated mathematical formulation. For this reason, only recently the value of Germain’s results was appreciated (see dell’Isola & Seppecher (2010)). Second gradient constitutive equations have been widely recognized to be essential in describing interface phenomena in phase-transition. Indeed, at the interface between different fluid phases, contact actions are not, because of long range molecular interactions, falling in the theoretical framework established by Cauchy. This circumstance has been recognized already by de Gennes(1981) (see also dell’Isola *et al.* (1996) and dell’Isola *et al.* (1995) and references there cited). More recently also second gradient constitutive equations for solids and porous media are being considered of interest (see e.g. Triantafyllidis & Bardenhagen (1996), dell’Isola *et al.* (2009b), Sciarra *et al.* (2008) and Madeo *et al.* (2008)). Aifantis (2003) showed that second gradient models are of great use also in the theory of plasticity, and the same holds true when continuum mechanics is used as a conceptual basis to describe, by means of numerical methods, damage modelling (see e.g. Yang and Misra (2010))

Many controversies which arose in the past about the importance and use of second gradient models concerned the physical interpretation of required boundary conditions and the need of establishing measurement procedures for second gradient constitutive parameters. The first issue arises whenever a novel theory is introduced by means of the least action principle or by means of Hamilton-Rayleigh principle or by means of the principle of virtual work. The needed interpretation of the obtained boundary conditions, has been, in our opinion,

satisfactorily given by Germain. In this paper, we propose to address the second issue and we study plane waves in second gradient solids and their reflection and transmission at planar surfaces in which displacement and its normal derivative may suffer a jump. Our aim is to start, for second gradient solids, to generalize the classical study of wave propagation which, for standard first gradient elastic media, is presented e.g. in Guyader (2006) and Harris (2004). Indeed, interesting boundary layer phenomena can be accounted for by second gradient models and these boundary phenomena may greatly influence wave propagation, transmission and reflection. To our knowledge, only in Toupin (1962) such a study has been initiated, even if only for a particular class of second gradient continua: those for which double contact forces reduce to contact couples. We prove that second gradient constitutive parameters determine, in a measurable manner, how planar waves behave at considered discontinuity surfaces. The novel results presented here can be the basis of experimental procedures to estimate some of second gradient constitutive parameters. Indeed, we show that for two kinds of boundary conditions the reflection and transmission coefficients remarkably depend on second gradient elastic moduli and that this dependence is increased when the frequency of the incident wave increases. Further investigations need to be directed towards a careful study of the influence of second gradient elastic moduli on the dependence on frequency of transmission and reflection coefficients. Moreover, the problem of extending the presented results to the case of more general boundary conditions and to wave propagation in porous media should also be addressed.

2 Mechanical energy transport in second gradient continua

In this section we deduce, starting from the appropriate equation of motion, the mechanical energy conservation law for a three-dimensional second gradient continuum. Similar results can be found in Casal & Gouin (1985) for second gradient fluids.

Let $\chi : B \times (0, T) \rightarrow \mathbb{R}^3$ be the placement map which, at any instant t , associates to any material particle $\mathbf{X} \in B$ its position in the physical space. The displacement field is then defined as $\mathbf{u}(\mathbf{X}, t) := \chi(\mathbf{X}, t) - \mathbf{X}$. We set $\mathbf{F} := \nabla \chi$ and we denote by $\boldsymbol{\varepsilon} := (\mathbf{F}^T \cdot \mathbf{F} - \mathbf{I})/2$ the classical Green-Lagrange deformation tensor. Let ρ be the mass per unit volume of the considered continuum in its reference configuration, we introduce, by means of

$$\mathcal{E} = \frac{1}{2} \rho (\dot{\mathbf{u}})^2 + \Psi(\boldsymbol{\varepsilon}, \nabla \boldsymbol{\varepsilon}), \quad (1)$$

the total Lagrangian energy density of the considered second gradient continuum, as given by the sum of the kinetic and deformation energy, which we denote by Ψ . Here and in the sequel a superposed dot represents partial differentiation with respect to time, i.e. what is usually called the material time derivative. Moreover, we recall that, in absence of body forces, the equation of motion for

a second gradient continuum reads (see e.g. Germain (1973a), dell’Isola *et al.* (2009b) or Sciarra *et al.* (2008) for a variational deduction of the equations of motion for second gradient materials)¹

$$\operatorname{div} \left[\mathbf{F} \cdot \left(\frac{\partial \Psi}{\partial \boldsymbol{\varepsilon}} - \operatorname{div} \left(\frac{\partial \Psi}{\partial \nabla \boldsymbol{\varepsilon}} \right) \right) \right] = \rho \ddot{\mathbf{u}} \quad (2)$$

Differentiating Eq. (1) with respect to time and using Eq. (2), it can be shown that²

$$\frac{\partial \mathcal{E}}{\partial t} + \operatorname{div} \left[-\dot{\mathbf{u}} \cdot \mathbf{F} \cdot \left(\frac{\partial \Psi}{\partial \boldsymbol{\varepsilon}} - \operatorname{div} \left(\frac{\partial \Psi}{\partial \nabla \boldsymbol{\varepsilon}} \right) \right) - \left((\nabla \dot{\mathbf{u}})^T \cdot \mathbf{F} \right) : \frac{\partial \Psi}{\partial \nabla \boldsymbol{\varepsilon}} \right] = 0. \quad (3)$$

In the calculations for obtaining Eq. (3) we used the fact that $\boldsymbol{\varepsilon}$ is a second order symmetric tensor, that $\nabla \boldsymbol{\varepsilon}$ is a third order tensor symmetric with respect to its first two indices and that $\nabla \mathbf{F}$ is a third order tensor symmetric with respect to its last two indices. Thus this last equation represents the Lagrangian form of energy balance for a second gradient 3D continuum in the general non-linear case.

We now want to focus our attention to the particular case of linear elasticity in order to study linear plane waves in second gradient 3D continua. To this purpose, we note that, when linearising in the neighbourhood of a stress-free reference configuration, the gradient of placement \mathbf{F} in Eq. (3) is substituted by the identity matrix and that the equation of motion and mechanical energy balance for a second gradient continuum respectively reduce to

$$\operatorname{div} [\mathbf{S} - \operatorname{div} \mathbf{P}] = \rho \ddot{\mathbf{u}}, \quad \frac{\partial \mathcal{E}}{\partial t} + \operatorname{div} \left[-\dot{\mathbf{u}} \cdot (\mathbf{S} - \operatorname{div} \mathbf{P}) - (\nabla \dot{\mathbf{u}})^T : \mathbf{P} \right] = 0, \quad (4)$$

where, following the nomenclature of Germain, \mathbf{S} and \mathbf{P} are the linearised Piola-Kirchhoff first and second gradient stress tensors respectively. In order to lighten the notation, however, we will refer to these two tensors simply as stress and hyper-stress tensor respectively. It is well known that in the case of isotropic material $\mathbf{S} = 2\mu \mathbf{E} + \lambda (\operatorname{tr} \mathbf{E}) \mathbf{I}$, where $\mathbf{E} = (\nabla \mathbf{u} + (\nabla \mathbf{u})^T)/2$ is the linearised Green-Lagrange deformation tensor and λ and μ are the so-called Lamé coefficients. As for the hyper-stress third order tensor \mathbf{P} , it can be shown (see e.g. dell’Isola *et al.* (2009b)) that in the case of isotropic materials it takes the following simplified form³

$$\begin{aligned} \mathbf{P} = & c_2 \left[2\mathbf{I} \otimes \operatorname{div} \mathbf{E} + (\mathbf{I} \otimes \nabla (\operatorname{tr} \mathbf{E}))^{T_{23}} + \nabla (\operatorname{tr} \mathbf{E}) \otimes \mathbf{I} \right] + c_3 \mathbf{I} \otimes \nabla (\operatorname{tr} \mathbf{E}) \\ & + 2c_5 \left[(\mathbf{I} \otimes \operatorname{div} \mathbf{E})^{T_{23}} + \operatorname{div} \mathbf{E} \otimes \mathbf{I} \right] + 2c_{11} \nabla \mathbf{E} + 4c_{15} (\nabla \mathbf{E})^{T_{12}}, \end{aligned} \quad (5)$$

¹The symbol *div* stands for the usual divergence operator, e.g. $(\operatorname{div} \mathbf{A})_{ij} = \mathbf{A}_{ijk,k}$. Here and in the sequel we adopt Einstein summation convention over repeated indices. The symbol ∇ stands for the usual gradient operator, e.g. $(\nabla \mathbf{A})_{ijk} = \mathbf{A}_{ij,k}$. A central dot indicates a simple contraction between two tensors of any order, e.g. $(\mathbf{A} \cdot \mathbf{B})_{ijhk} = \mathbf{A}_{ijp} \mathbf{B}_{phk}$

²A double dot indicates a double contraction between two tensors of any order, e.g. $(\mathbf{A} : \mathbf{B})_{ij} = \mathbf{A}_{ihk} \mathbf{B}_{khj}$.

³We define the transposition operations of a third order tensor as $A_{ijk}^{T_{23}} = A_{ikj}$ and $A_{ijk}^{T_{12}} = A_{jik}$ and the symbol \otimes as the usual tensor product operation between two tensors of any order (e.g. $(A \otimes B)_{ijhk} = A_{ij} B_{hk}$)

where c_2, c_3, c_5, c_{11} and c_{15} are constants depending on the material properties of the considered second gradient continuum. As it will be seen to be useful later on, we define the following coefficients

$$\Lambda := c_3 + 2(c_5 + c_{15}) + 4c_2, \quad M := c_{11} + c_{15} + c_5, \quad (6)$$

which parallel the first gradient Lamé coefficients λ and μ .

3 Dispersion Formulas

Let us now consider a wave travelling in the considered second gradient continuum. We denote by x_1 the axis of a reference frame the direction of which coincides with the propagation direction and by x_2 and x_3 the other two directions forming a Cartesian basis with x_1 . We assume that the displacement vector has three non-vanishing components depending only on the x_1 coordinate and on time, i.e. $\mathbf{u}(x_1, t) = (u_1(x_1, t), u_2(x_1, t), u_3(x_1, t))$. In the following we will say that we are in presence of a unidirectional wave propagation. With this assumption it is easy to show that the associated matrix form of the linearised deformation tensor reads

$$\mathbf{E} = \begin{pmatrix} u_1' & u_2'/2 & u_3'/2 \\ u_2'/2 & 0 & 0 \\ u_3'/2 & 0 & 0 \end{pmatrix} \quad (7)$$

where we clearly denote by an apex the partial differentiation with respect to the space variable x_1 . Using (7) to calculate the stress and hyper-stress tensors $\mathbf{S} = 2\mu\mathbf{E} + \lambda(\text{tr}\mathbf{E})\mathbf{I}$ and \mathbf{P} (see Eqs. (5) and (6)), the equation of motion (4)₁ takes the following form

$$(\lambda + 2\mu)u_1'' - (\Lambda + 2M)u_1'''' = \rho\ddot{u}_1, \quad (8)$$

$$\mu u_2'' - M u_2'''' = \rho\ddot{u}_2, \quad \mu u_3'' - M u_3'''' = \rho\ddot{u}_3. \quad (9)$$

We notice that the equations of motion obtained in this unidirectional wave propagation are completely uncoupled due to the particular constitutive relations assumed for isotropic, linear elastic, second gradient continua. Moreover, the conservation of energy (4)₂ gives $\partial\mathcal{E}/\partial t + H' = 0$ where we denote

$$H := -(\lambda + 2\mu)(u_1'\dot{u}_1) - \mu(u_2'\dot{u}_2) - \mu(u_3'\dot{u}_3) + (\Lambda + 2M)(u_1'''\dot{u}_1 - u_1''\dot{u}_1') + M(u_2'''\dot{u}_2 - u_2''\dot{u}_2') + M(u_3'''\dot{u}_3 - u_3''\dot{u}_3'), \quad (10)$$

the energy flux in the considered particular case. We also remark that M and $\Lambda + 2M$ are positive due to definite-positiveness of the internal energy (see e.g. dell'Isola *et al.* (2009b)). We now assume that the displacement field admits a classical wave solution in the form

$$\mathbf{u} = \begin{pmatrix} u_1 \\ u_2 \\ u_3 \end{pmatrix} = \begin{pmatrix} \alpha_1 \\ \alpha_2 \\ \alpha_3 \end{pmatrix} e^{i(\omega t - kx_1)} \quad (11)$$

where the eigenvector $(\alpha_1, \alpha_2, \alpha_3)$ gives the longitudinal and transversal amplitudes of the considered wave, ω is the positive real frequency and k its wave number. Using this wave form for \mathbf{u} in the equations of motion for longitudinal and transversal displacement (8) and (9) we get the following dispersion relations for a second gradient continuum

$$\begin{aligned} (\Lambda + 2M)k_1^4 + (\lambda + 2\mu)k_1^2 - \rho\omega^2 &= 0, \\ Mk_2^4 + \mu k_2^2 - \rho\omega^2 &= 0, \quad Mk_3^4 + \mu k_3^2 - \rho\omega^2 = 0, \end{aligned}$$

where k_1 is the wave number relative to the eigenvector $(1, 0, 0)$, k_2 and k_3 are the wave numbers relative to the eigenvectors $(0, 1, 0)$ and $(0, 0, 1)$ respectively. Since we are dealing with isotropic media, the two transverse dispersion relations coincide: in what follows we therefore shall ignore the last dispersion relation.

Because of isotropy, the waves arising in considered medium can be either purely transversal or purely longitudinal. We now look for non-dimensional form of these relations by setting: $k_1 = k_l \tilde{k}_l$, $\omega = \omega_l \tilde{\omega}$ for longitudinal waves and $k_2 = k_t \tilde{k}_t$, $\omega = \omega_t \tilde{\omega}$ for transverse waves. Here k_l (or k_t), ω_l (or ω_t) are characteristic values of the wave number and of the frequency for longitudinal (or transverse) waves respectively; moreover, \tilde{k}_l , \tilde{k}_t and $\tilde{\omega}$ are the corresponding dimensionless variables. This leads to

$$\begin{aligned} \frac{(\Lambda + 2M)}{(\lambda + 2\mu)} k_l^2 \tilde{k}_l^4 + \tilde{k}_l^2 - \frac{\rho}{(\lambda + 2\mu)} \frac{\omega_l^2}{k_l^2} \tilde{\omega}^2 &= 0, \\ \frac{M}{\mu} k_t^2 \tilde{k}_t^4 + \tilde{k}_t^2 - \frac{\rho}{\mu} \frac{\omega_t^2}{k_t^2} \tilde{\omega}^2 &= 0. \end{aligned}$$

To our knowledge, similar dispersion formulas for a particular class of second gradient materials has been already studied only by Toupin (1962). We finally choose k_l^2 and k_t^2 to be such that the coefficients of $\tilde{\omega}^2$ in the two dispersion relations are both equal to one and hence we get

$$k_l^2 = \rho\omega_l^2/(\lambda + 2\mu) \quad k_t^2 = \rho\omega_t^2/\mu. \quad (12)$$

The dispersion relations thus reduce to

$$\epsilon_l^2 \tilde{k}_l^4 + \tilde{k}_l^2 - \tilde{\omega}^2 = 0, \quad \epsilon_t^2 \tilde{k}_t^4 + \tilde{k}_t^2 - \tilde{\omega}^2 = 0, \quad (13)$$

where we set

$$\epsilon_l^2 = \frac{\rho(\Lambda + 2M)}{(\lambda + 2\mu)^2} \omega_l^2, \quad \epsilon_t^2 = \frac{\rho M}{\mu^2} \omega_t^2.$$

The relationships between the dimensionless wave number and frequency is thus easily recovered both for longitudinal and transverse waves by solving the bi-quadratic equations (13):

$$\tilde{k}_l = \pm \sqrt{\frac{-1 \pm \sqrt{1 + 4\epsilon_l^2 \tilde{\omega}^2}}{2\epsilon_l^2}}, \quad \tilde{k}_t = \pm \sqrt{\frac{-1 \pm \sqrt{1 + 4\epsilon_t^2 \tilde{\omega}^2}}{2\epsilon_t^2}}.$$

If we consider the positive real numbers

$$\tilde{k}_l^p = \sqrt{\frac{-1 + \sqrt{1 + 4\epsilon_l^2 \tilde{\omega}^2}}{2\epsilon_l^2}}, \quad \tilde{k}_l^s = \sqrt{\frac{1 + \sqrt{1 + 4\epsilon_l^2 \tilde{\omega}^2}}{2\epsilon_l^2}}, \quad (14)$$

$$\tilde{k}_t^p = \sqrt{\frac{-1 + \sqrt{1 + 4\epsilon_t^2 \tilde{\omega}^2}}{2\epsilon_t^2}}, \quad \tilde{k}_t^s = \sqrt{\frac{1 + \sqrt{1 + 4\epsilon_t^2 \tilde{\omega}^2}}{2\epsilon_t^2}}, \quad (15)$$

the four roots associated to longitudinal waves are clearly $\pm\tilde{k}_l^p$, $\pm i\tilde{k}_l^s$, and analogously we have for the transverse waves the four roots $\pm\tilde{k}_t^p$, $\pm i\tilde{k}_t^s$. It is clear that one can derive the corresponding dimensional quantities k_1^p and k_1^s (for longitudinal waves) and k_2^p and k_2^s (for transverse waves) just multiplying the non-dimensional roots \tilde{k}_l and \tilde{k}_t by k_l and k_t respectively (see eqs. (12)). As we will see in more detail later on, the roots \tilde{k}^p are associated to *propagative waves* which are a second gradient generalization of the waves propagating in a first gradient material, while the roots \tilde{k}^s are the so-called *standing waves* (or evanescent waves) (see e.g. Guyader (2006), Harris (2004), Carvalho (2001)) and are peculiar of second gradient models. These standing waves will be seen to play a significant role close to material discontinuity surfaces in second gradient continua where phenomena of reflection and transmission may occur. Indeed, there are other physical situations in which standing waves may appear. For instance, Ouisse & Guyader (2003) showed that this may occur when studying coupling between the transversal displacement u and the longitudinal displacement w in one-dimensional beams.

4 Natural and kinematical boundary conditions at surfaces where displacement or normal derivative of displacement may be discontinuous

The problem of finding boundary conditions to be imposed at discontinuity surfaces is always challenging for the modelling of any physical phenomenon. Indeed, the only possible method which leads to surely well-posed boundary conditions, compatible with the obtained bulk equations of motion, is to use a variational principle. This is the case also when looking for the correct set of boundary conditions associated to the motion of a second gradient continuum. We just recall here the boundary (or jump) conditions found for a second gradient material in dell'Isola *et al.* (2009b) or Sciarra *et al.* (2008). The boundary conditions on the considered discontinuity surface S , in absence of external surface and line actions, can be deduced from the following duality conditions

$$[[\mathbf{t} \cdot \delta \mathbf{u}]] = 0, \quad [[\boldsymbol{\tau} \cdot (\delta \mathbf{u})_n]] = 0, \quad [[\mathbf{f} \cdot \delta \mathbf{u}]] = 0. \quad (16)$$

The first two of these conditions are valid on S while the last one is valid on the edges of S , if any. In the previous formulas (16) we set

$$\begin{aligned}\mathbf{t} &:= \left[\mathbf{F} \cdot \left(\frac{\partial \Psi}{\partial \varepsilon} - \operatorname{div} \left(\frac{\partial \Psi}{\partial \nabla \varepsilon} \right) \right) \right] \cdot \mathbf{n} - \operatorname{div}^S \left(\mathbf{F} \cdot \frac{\partial \Psi}{\partial \nabla \varepsilon} \cdot \mathbf{n} \right), \\ \boldsymbol{\tau} &:= \left(\mathbf{F} \cdot \frac{\partial \Psi}{\partial \nabla \varepsilon} \cdot \mathbf{n} \right) \cdot \mathbf{n}, \quad \mathbf{f} := \left(\mathbf{F} \cdot \frac{\partial \Psi}{\partial \nabla \varepsilon} \cdot \mathbf{n} \right) \cdot \boldsymbol{\nu}.\end{aligned}$$

Moreover, \mathbf{n} is the unit normal vector to the surface S , div^S stands for the surface divergence operator on S , if the edge is regarded as the border of a surface then $\boldsymbol{\nu}$ is the normal vector to the considered edge which is tangent to the surface, $\delta \mathbf{u}$ is the variation of the displacement field and $(\delta \mathbf{u})_n := \nabla(\delta \mathbf{u}) \cdot \mathbf{n}$ stands for the normal derivative of the variation of the displacement field. Finally, given a quantity a defined everywhere and having continuous traces a^+ and a^- on the two sides of S respectively, we have set $[[a]] := a^+ - a^-$ (we use the same symbol for the jump across edges).

When choosing arbitrary displacement variation $\delta \mathbf{u}$ continuously varying through S and arbitrary normal derivative $(\delta \mathbf{u})_n$ continuously varying through S in equations (16), one gets a particular set of *natural jump conditions*, which can be interpreted as the vanishing jump of internal surface forces ($[[\mathbf{t}]] = 0$), the vanishing jump of internal surface *double forces* ($[[\boldsymbol{\tau}]] = 0$) and the vanishing jump of internal line actions ($[[\mathbf{f}]] = 0$) respectively (see Germain (1973a) and Germain (1973b) for the first introduction of the concept of contact double force). Indeed, if it happens that the displacement field, due to a particular constraint, verifies the particular equation $\delta \mathbf{u}^- = \delta \mathbf{u}^+ =: \delta \mathbf{u}$ (vanishing jump of the displacement field), and $\delta \mathbf{u}$ is arbitrary, then in order to fulfil conditions (16)₁ and (16)₃ one must require that also the jumps of the dual quantities to $\delta \mathbf{u}$ (i.e. surface forces and line forces) are vanishing. Analogously, if the normal derivative of displacement is assigned to be equal on both sides of S and this common value is arbitrary, then in order eq. (16)₂ to be verified one must also impose continuity of internal double forces. Conditions of the type $\delta \mathbf{u}^- = \delta \mathbf{u}^+$, or any similar relationship among $\delta \mathbf{u}^\pm$ and $(\delta \mathbf{u})_n^\pm$, are called *kinematical boundary conditions*. Once the kinematical boundary conditions are chosen, the associated dual conditions necessary and sufficient to fulfil duality conditions (16), are called natural boundary conditions associated to the chosen kinematical ones. Therefore, in addition to those previously discussed, other kinematical choices are possible in the previously formulated duality conditions, these choices being indicated by the admissible kinematics of the considered system or, in simpler words, by the considered phenomenology. We discuss here some kinematical constraints for second gradient continua, which we call *generalized internal clamp*, *generalized internal hinge* and *generalized internal roller* and the natural boundary conditions associated to them.

- *Generalized internal clamp.*

We define this constraint imposing the continuity of both the displacement \mathbf{u} and the normal derivative of displacement $\nabla \mathbf{u} \cdot \mathbf{n}$ (and therefore of the

test function $\delta \mathbf{u}$ and of its normal derivative $(\delta \mathbf{u})_n$ at the discontinuity surface S which from now on we assume to be regular (i.e S has no edges). As already noticed, in this case boundary conditions are

$$[[\mathbf{u}]] = 0, \quad [[\nabla \mathbf{u} \cdot \mathbf{n}]] = 0, \quad [[\mathbf{t}]] = 0, \quad [[\boldsymbol{\tau}]] = 0. \quad (17)$$

If we consider unidirectional wave propagation, and if we choose a flat surface S such that its normal is given by $\mathbf{n} = (1, 0, 0)$, then the jump conditions (17) particularize into

$$\begin{aligned} [[u_1]] = 0, \quad [[u'_1]] = 0, \quad [[(\lambda + 2\mu)u'_1 - (\Lambda + 2M)u''_1]] = 0, \quad [[(\Lambda + 2M)u''_1]] = 0, \\ [[u_2]] = 0, \quad [[u'_2]] = 0, \quad [[(\mu u'_2 - Mu''_2)]] = 0, \quad [[Mu''_2]] = 0, \quad (18) \\ [[u_3]] = 0, \quad [[u'_3]] = 0, \quad [[(\mu u'_3 - Mu''_3)]] = 0, \quad [[Mu''_3]] = 0. \end{aligned}$$

- *Generalized internal hinge*

We define the constraint of generalized internal hinge at surface S imposing continuity of displacement (which as before implies continuity of generalized force \mathbf{t}) and assuming that $(\delta \mathbf{u})_n^+$ and $(\delta \mathbf{u})_n^-$ can independently take arbitrary values on the two sides of S . These last conditions, together with the duality condition (16)₂, imply that the double forces must be separately vanishing on the two sides of S . In formulas, the four conditions for a generalized hinge are

$$[[\mathbf{u}]] = 0, \quad [[\mathbf{t}]] = 0, \quad \boldsymbol{\tau}^+ = 0, \quad \boldsymbol{\tau}^- = 0. \quad (19)$$

In the considered unidirectional wave propagation these conditions reduce to

$$\begin{aligned} [[u_1]] = 0, \quad [[(\lambda + 2\mu)u'_1 - (\Lambda + 2M)u''_1]] = 0, \quad ((\Lambda + 2M)u''_1)^\pm = 0, \\ [[u_2]] = 0, \quad [[(\mu u'_2 - Mu''_2)]] = 0, \quad (Mu''_2)^+ = (Mu''_2)^- = 0, \quad (20) \\ [[u_3]] = 0, \quad [[(\mu u'_3 - Mu''_3)]] = 0, \quad (Mu''_3)^+ = (Mu''_3)^- = 0. \end{aligned}$$

- *Generalized 3D internal roller*

We define the last kind of kinematical constraint considered in this paper which we call generalized roller and which is defined in such a way that it allows independently arbitrary displacements on both sides of S (which implies separately $\delta \mathbf{u}^+$ and $\delta \mathbf{u}^-$ to be arbitrary) and such that the normal derivative of displacement is continuous through S (i.e. $[[\nabla \mathbf{u} \cdot \mathbf{n}]] = 0$). The first condition together with eq. (16)₁ implies that the generalized force must be separately vanishing on both sides of S , while the second condition implies continuity of double forces through S . Hence the four conditions for a generalized roller are

$$\mathbf{t}^+ = 0, \quad \mathbf{t}^- = 0, \quad [[\nabla \mathbf{u} \cdot \mathbf{n}]] = 0, \quad [[\boldsymbol{\tau}]] = 0. \quad (21)$$

It can be shown that in the considered unidirectional propagation case these equations simplify into

$$\begin{aligned}
((\lambda + 2\mu)u'_1 - (\Lambda + 2M)u''_1)^\pm &= 0, & [[u'_1]] &= 0, & [(\Lambda + 2M)u''_1] &= 0, \\
(\mu u'_2 - M u''_2)^+ &= (\mu u'_2 - M u''_2)^- = 0, & [[u'_2]] &= 0, & [[M u''_2]] &= 0, \\
(\mu u'_3 - M u''_3)^+ &= (\mu u'_3 - M u''_3)^- = 0, & [[u'_3]] &= 0, & [[M u''_3]] &= 0.
\end{aligned} \tag{22}$$

As occurs for the dispersion relations, also for the boundary conditions, we can notice that in the considered linear-elastic case, they are completely uncoupled in the longitudinal and transversal displacement due to isotropy and to the fact that the displacement only depends on the x_1 variable.

5 Transmission and reflection at discontinuity surfaces

Let us now recall that we are considering a flat discontinuity surface S inside the considered second gradient continuum. We denote by \mathbf{n} the unit normal to S and we choose the fixed reference frame in such a way that \mathbf{n} points in the x_1 direction: we are assuming that the vector \mathbf{n} is always the same at any point of S (see Fig.1). As before, we denote by x_2 and x_3 the other two directions of the fixed reference frame forming a Cartesian basis with x_1 . Using

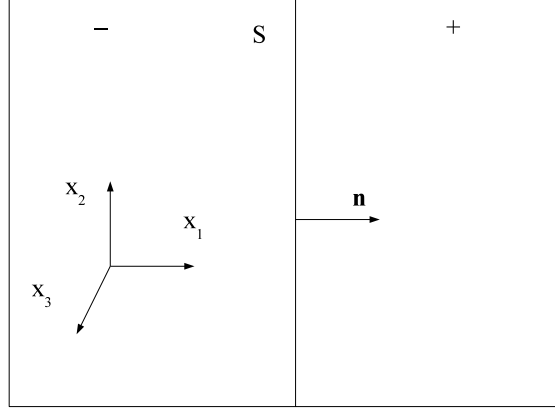


Figure 1: Domain with flat discontinuity surface

the equations of motion (8) and (9) on both sides of S and the linearised jump conditions (18), (20) or (22), we are able to describe the motion of two different isotropic, linear-elastic second gradient continua which are in contact through the discontinuity surface S and considering three different constraints at this

surface (generalized internal clamp, generalized internal hinge and generalized internal roller). Nevertheless, in this paper we limit ourselves to the case of two second gradient continua with the same material properties (same first and second gradient elasticity parameters) in contact through the surface S at which we impose the three generalized types of constraints discussed before.

Let us start by studying the case of longitudinal waves (the involved field is then the one we previously denoted by u_1) impacting at the interface S and then we will repeat the reasoning for transverse waves (the involved field is then u_2): this is allowed to the fact that the obtained problem is completely uncoupled with respect to longitudinal and transversal displacements.

Then let us consider an incident longitudinal wave u_i^l propagating in the x_1 direction and defined as

$$u_i^l = \alpha_i^l e^{i(\omega t - k_1^p x_1)},$$

where α_i^l is the amplitude of the incident (subscript i), longitudinal (superscript l) wave which we assume to be assigned, ω is the real positive frequency of such an incident wave and, $k_1^p = \tilde{k}_1^p k_l$ (see eqs. (14)₁ and 12) is the positive real wave number associated to the propagating wave travelling in the x_1 direction. When this wave reaches the interface S reflection and transmission phenomena take place (see Fig. 2). We call u_r^l and u_t^l the reflected and transmitted longitudinal

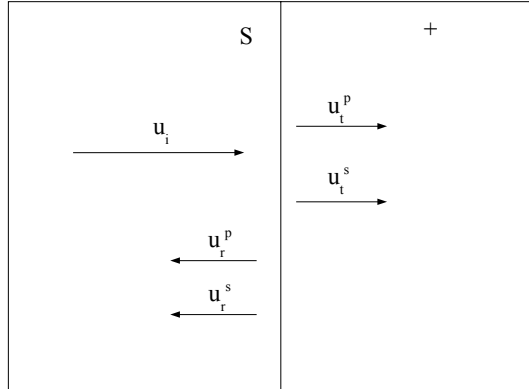


Figure 2: Reflected and transmitted waves

wave respectively. According to the geometry of the considered problem and to equations (14) the reflected wave propagates always in the x_1 direction and take the following form

$$u_r^l = u_r^{lp} + u_r^{ls} = \alpha_r^l e^{i(\omega t + k_1^p x_1)} + \beta_r^l e^{i(\omega t - i k_1^s x_1)},$$

where α_r^l is the amplitude of the propagative reflected wave travelling in the $-x_1$ direction and β_r^l is the amplitude of the standing reflected wave. Note

that $k_1^s = \tilde{k}_1^s k_l$ (see eqs. (14)₂ and (12)) is the positive real wave number associated to the standing wave and that the standing reflected wave vanishes as x_1 approaches $-\infty$. Analogously, the transmitted wave is may be represented by

$$u_t^l = u_t^{lp} + u_t^{ls} = \alpha_t^l e^{i(\omega t - k_1^p x_1)} + \beta_t^l e^{i(\omega t + i k_1^s x_1)},$$

where α_t^l is the amplitude of the propagative transmitted wave travelling in the x_1 direction and β_t^l is the amplitude of the standing transmitted wave. Note that the standing transmitted wave vanishes as x_1 approaches $+\infty$. We remark that, among the two possible standing reflected (transmitted) waves we did not consider that one which diverges as $x_1 \rightarrow -\infty$ ($x_1 \rightarrow +\infty$), as we assume a Sommerfeld-type condition at infinity.

As we want to deal with dimensionless quantities, we introduce the non-dimensional counterpart of these displacements by considering the non-dimensional variables $\tilde{t} = \omega_l t$ and $\tilde{x}_1 = k_l x_1$, where the characteristic quantities ω_l and k_l have been defined in section 3. We can then introduce the non-dimensional form of the considered displacements as

$$\tilde{u}_i^l := \frac{u_i^l}{\alpha_i^l} = e^{i(\tilde{\omega}\tilde{t} - \tilde{k}_i^p \tilde{x}_1)}, \quad (23)$$

$$\tilde{u}_r^l := \frac{u_r^l}{\alpha_i^l} = \tilde{\alpha}_r^l e^{i(\tilde{\omega}\tilde{t} + \tilde{k}_i^p \tilde{x}_1)} + \tilde{\beta}_r^l e^{i(\tilde{\omega}\tilde{t} - i\tilde{k}_i^s \tilde{x}_1)}, \quad (24)$$

$$\tilde{u}_t^l := \frac{u_t^l}{\alpha_i^l} = \tilde{\alpha}_t^l e^{i(\tilde{\omega}\tilde{t} - \tilde{k}_i^p \tilde{x}_1)} + \tilde{\beta}_t^l e^{i(\tilde{\omega}\tilde{t} + i\tilde{k}_i^s \tilde{x}_1)}, \quad (25)$$

where clearly we set $\tilde{\alpha}_r^l = \alpha_r^l/\alpha_i^l$, $\tilde{\beta}_r^l = \beta_r^l/\alpha_i^l$, $\tilde{\alpha}_t^l = \alpha_t^l/\alpha_i^l$ and $\tilde{\beta}_t^l = \beta_t^l/\alpha_i^l$, where \tilde{k}_i^p and \tilde{k}_i^s are given by Eqs. (14) and where the dimensionless frequency $\tilde{\omega} = \omega/\omega_l$ has been defined in section 3.

It is clear that once the frequency and the first and second gradient elasticity parameters are given, the only unknowns of the reflection/transmission problem are the four amplitudes $\tilde{\alpha}_r^l$, $\tilde{\beta}_r^l$, $\tilde{\alpha}_t^l$ and $\tilde{\beta}_t^l$. These four scalar unknowns can be found for each of the three types of constraints introduced by considering Eqs. (18)₁, (20)₁ and (22)₁ respectively which only involve the longitudinal displacement. In conclusion, if we notice that here the first component of $[[\mathbf{u}]]$ takes the form $[[u_1]] = u_i^l - u_r^l - u_t^l$, and if we replace the wave form of the longitudinal displacement field in the non-dimensional version of equations (18)₁, (20)₁ and (22)₁ at $x_1 = 0$, we can finally recover the expression of the four amplitudes for each of the three types of constraints considered.

- *Generalized internal clamp.*

As for the generalized internal clamp, the non-dimensional jump conditions (18) in the considered case in which the two continua on the two sides of S have the same material properties simply read

$$[[\tilde{u}_1]] = 0, \quad [[\tilde{u}'_1]] = 0, \quad [[\tilde{u}'_1 - \epsilon_l^2 \tilde{u}'''_1]] = 0, \quad [[\tilde{u}''_1]] = 0,$$

where, with a slight abuse of notation, we indicate with an apex the derivation operation with respect to the dimensionless space variable \tilde{x}_1 . Replacing the aforementioned wave form for non-dimensional displacements in these boundary conditions we calculate the following non-dimensional amplitudes for longitudinal waves

$$\tilde{\alpha}_r^l = 0, \quad \tilde{\beta}_r^l = 0, \quad \tilde{\alpha}_t^l = 1, \quad \tilde{\beta}_t^l = 0. \quad (26)$$

This means that in the case of a perfect internal clamp at the surface S , the incident wave is completely transmitted. This result is not astonishing if we think that the two materials on both sides of S have been chosen to have the same material properties: indeed, it is as if there were no discontinuity at all and hence the incident wave proceeds unperturbed across the surface S .

- *Generalized internal hinge.*

As for the generalized internal hinge between two continua with the same material properties, the non-dimensional form of jump conditions (20) reads

$$[[\tilde{u}_1]] = 0, \quad [[\tilde{u}'_1 - \epsilon_l^2 \tilde{u}'''_1]] = 0, \quad (\tilde{u}'_1)^+ = 0, \quad (\tilde{u}'_1)^- = 0,$$

Using the considered wave form for displacements in these boundary conditions, the calculated non-dimensional amplitudes take the form

$$\begin{aligned} \tilde{\alpha}_r^l &= \frac{i\tilde{k}_l^p [1 - \epsilon_l^2 (\tilde{k}_l^s)^2]}{(\tilde{k}_l^p + i\tilde{k}_l^s)(-i + \epsilon_l^2 \tilde{k}_l^p \tilde{k}_l^s)}, & \tilde{\beta}_r^l &= \frac{(\tilde{k}_l^p)^2 [1 + \epsilon_l^2 (\tilde{k}_l^p)^2]}{\tilde{k}_l^s (\tilde{k}_l^p + i\tilde{k}_l^s)(-i + \epsilon_l^2 \tilde{k}_l^p \tilde{k}_l^s)}, \\ \tilde{\alpha}_t^l &= \frac{\tilde{k}_l^s [1 + \epsilon_l^2 (\tilde{k}_l^p)^2]}{(\tilde{k}_l^p + i\tilde{k}_l^s)(-i + \epsilon_l^2 \tilde{k}_l^p \tilde{k}_l^s)}, & \tilde{\beta}_t^l &= \frac{(\tilde{k}_l^p)^2 [1 + \epsilon_l^2 (\tilde{k}_l^p)^2]}{\tilde{k}_l^s (\tilde{k}_l^p + i\tilde{k}_l^s)(-i + \epsilon_l^2 \tilde{k}_l^p \tilde{k}_l^s)}. \end{aligned} \quad (27)$$

- *Generalized 3D internal roller.*

Finally, if we consider a generalized roller between two continua with the same material properties, the non-dimensional form of jump conditions (22) reads

$$[[\tilde{u}'_1]] = 0, \quad (\tilde{u}'_1 - \epsilon_l^2 \tilde{u}'''_1)^+ = 0, \quad (\tilde{u}'_1 - \epsilon_l^2 \tilde{u}'''_1)^- = 0, \quad [[\tilde{u}''_1]] = 0,$$

Using the considered wave form for dimensionless displacements in these boundary conditions we get the following values for non-dimensional amplitudes

$$\begin{aligned} \tilde{\alpha}_r^l &= \frac{k_l^s [1 + \epsilon_l^2 (\tilde{k}_l^p)^2]}{(\tilde{k}_l^p + i\tilde{k}_l^s)(-i + \epsilon_l^2 \tilde{k}_l^p \tilde{k}_l^s)}, & \tilde{\beta}_r^l &= \frac{(\tilde{k}_l^p)^2 [1 + \epsilon_l^2 (\tilde{k}_l^p)^2]}{\tilde{k}_l^s (\tilde{k}_l^p + i\tilde{k}_l^s)(-i + \epsilon_l^2 \tilde{k}_l^p \tilde{k}_l^s)}, \\ \tilde{\alpha}_t^l &= \frac{i\tilde{k}_l^p [-1 + \epsilon_l^2 (\tilde{k}_l^s)^2]}{(\tilde{k}_l^p + i\tilde{k}_l^s)(-i + \epsilon_l^2 \tilde{k}_l^p \tilde{k}_l^s)}, & \tilde{\beta}_t^l &= \frac{-(\tilde{k}_l^p)^2 [1 + \epsilon_l^2 (\tilde{k}_l^p)^2]}{\tilde{k}_l^s (\tilde{k}_l^p + i\tilde{k}_l^s)(-i + \epsilon_l^2 \tilde{k}_l^p \tilde{k}_l^s)}. \end{aligned} \quad (28)$$

Let us now consider the case of transverse waves travelling in the x_1 direction. As done for longitudinal waves, we introduce the incident transversal displacement as:

$$u_i^t = \alpha_i^t e^{i(\omega t - k_2^p x_1)},$$

where α_i^t is the amplitude of the incident transverse wave which we assume to be known and k_2^p is the wave number associated to a transverse wave propagating in the x_1 direction. We then call u_r^t and u_t^t the reflected and transmitted transverse wave respectively. According to the geometry of the considered problem the reflected and transmitted waves take the following form

$$u_r^t = u_r^{tp} + u_r^{ts} = \alpha_r^t e^{i(\omega t + k_2^p x_1)} + \beta_r^t e^{i(\omega t + i k_2^s x_1)},$$

where α_r^t is the amplitude of the propagative reflected wave travelling in the $-x_1$ direction and β_r^t is the amplitude of the standing reflected wave. Note that the standing reflected wave goes to zero as x_1 approaches $-\infty$. Moreover, the transmitted wave is defined as

$$u_t^t = u_t^{tp} + u_t^{ts} = \alpha_t^t e^{i(\omega t - k_2^p x_1)} + \beta_t^t e^{i(\omega t - i k_2^s x_1)},$$

The obtained equations for transversal waves are formally analogous to longitudinal ones, since one has just to replace \tilde{u}_1 with \tilde{u}_2 and all the subscripts and superscripts l with the subscripts and superscripts t respectively. Repeating the calculations performed for longitudinal waves, we can then calculate the four amplitudes $\tilde{\alpha}_r^t$, $\tilde{\beta}_r^t$, $\tilde{\alpha}_t^t$ and $\tilde{\beta}_t^t$ of the reflected and transmitted transverse waves for the three considered types of constraints imposed at the surface S .

6 Dependence of transmission and reflection coefficients on second gradient elastic moduli

In this section we will show plots displaying the reflection and transmission coefficients at discontinuity surfaces of the three types considered before as functions of second gradient elastic moduli. To do so, we start by noticing that owing to the fact that the problem is completely uncoupled in the longitudinal and transversal displacements, we can account separately for the energy fluxes of longitudinal and transversal waves. Moreover, due to the linearity of the problem in study, we can consider separate contributions for the fluxes of the incident, reflected and transmitted waves which, starting from expression (10), can be written in terms of the introduced non-dimensional variables respectively as

$$\begin{aligned} \tilde{H}_i^l(\tilde{x}_1, \tilde{t}) &= (\alpha_i^l)^2 k_l \omega_l (\lambda + 2\mu) \left[-(\tilde{u}_i^l)' \dot{\tilde{u}}_i^l + \epsilon_l^2 \left((\tilde{u}_i^l)''' \dot{\tilde{u}}_i^l - (\tilde{u}_i^l)'' (\dot{\tilde{u}}_i^l)' \right) \right], \\ \tilde{H}_r^l(\tilde{x}_1, \tilde{t}) &= (\alpha_i^l)^2 k_l \omega_l (\lambda + 2\mu) \left[-(\tilde{u}_r^l)' \dot{\tilde{u}}_r^l + \epsilon_l^2 \left((\tilde{u}_r^l)''' \dot{\tilde{u}}_r^l - (\tilde{u}_r^l)'' (\dot{\tilde{u}}_r^l)' \right) \right], \\ \tilde{H}_t^l(\tilde{x}_1, \tilde{t}) &= (\alpha_i^l)^2 k_l \omega_l (\lambda + 2\mu) \left[-(\tilde{u}_t^l)' \dot{\tilde{u}}_t^l + \epsilon_l^2 \left((\tilde{u}_t^l)''' \dot{\tilde{u}}_t^l - (\tilde{u}_t^l)'' (\dot{\tilde{u}}_t^l)' \right) \right], \end{aligned} \tag{29}$$

where we recall that, with a slight abuse of notation, the apex and the dot stand here for the derivation operations with respect to the introduced dimensionless space and time variables. The corresponding energy fluxes for transversal waves are formally analogous and are obtained from the previous ones just replacing everywhere the apex l with the apex t and the parameter ϵ_l with the parameter ϵ_t . In order to be able to calculate the reflection and transmission coefficients for the considered problem, we substitute in Eqs. (29) the wave forms (23), (24) and (25) for the displacements and we calculate the integrals over the period $2\pi/\tilde{\omega}$ of the introduced energy fluxes. It can be shown that, due to conservation of energy, these integrals do not depend on the space variable \tilde{x}_1 . Owing to this independence on the variable \tilde{x}_1 , in order to simplify calculations, we can simply introduce these integrals as

$$J_i^l = \int_0^T \tilde{H}_i^l(0, \tilde{t}) d\tilde{t}, \quad J_r^l = \int_0^T \tilde{H}_i^l(-\infty, \tilde{t}) d\tilde{t}, \quad J_t^l = \int_0^T \tilde{H}_i^l(+\infty, \tilde{t}) d\tilde{t}.$$

We are then finally able to introduce the reflection and transmission coefficients for longitudinal waves as

$$R_l := \frac{J_r^l}{J_i^l}, \quad T_l := \frac{J_t^l}{J_i^l},$$

which are such that $R_l + T_l = 1$. The reflection and transmission coefficients R_t and T_t for transversal waves are formally analogous.

We show in the following figures the behaviour of reflection and transmission coefficients in terms of the second gradient parameter ϵ , and of the frequency ω . These figures refer to both the longitudinal and transversal case: one has just to interpret ϵ as ϵ_l and ϵ_t respectively. In the plots, with an abuse of notation, ω stands for $\tilde{\omega}$.

Referring to Fig.3, we can note that, for very low frequencies (approaching to zero) and considering a generalized internal hinge at the discontinuity surface, the energy of the travelling wave is almost completely transmitted independently on the value of the second gradient parameter ϵ^2 . For higher frequencies, Fig.3 shows that the second gradient parameter starts to play a role with respect to the amount of energy which is reflected or transmitted. In particular, for frequencies increasing from 0 to 1, we can notice a gradual increase in the reflected energy: this increased amount of reflected energy is more evident for values of the second gradient parameter included in the interval $[0, 0.5]$. This behavior can be explained if one thinks that, for increasing frequencies, the wave length of the travelling wave decreases and becomes comparable to the characteristic length of the heterogeneities that are present in the material at a microscopic level. The described phenomenon is revealed by using a second gradient model which, though macroscopic in nature, allows for the description of some microscopic effects. The presence of heterogeneities at a microscopic level hence triggers the phenomenon of increasing the amount of reflected energy at the discontinuity surface. Hence, for frequencies lower than or equal to 1 we are able to detect this phenomenon of enhanced reflection, but the amount of

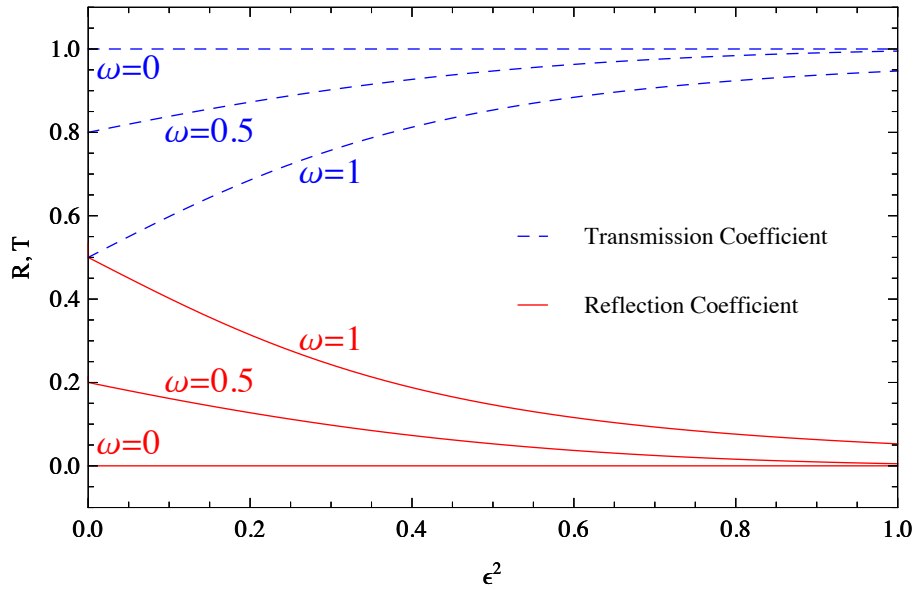


Figure 3: Reflection and transmission coefficients in presence of a generalized internal hinge for low-frequencies. The plots for the generalized internal roller are completely specular: the blue dashed lines must be referred to the reflection coefficient, while the red lines must be referred to the transmission coefficient.

reflected energy still remains lower with respect to the amount of the transmitted one for any value of the second gradient parameter. In this sense, the value of frequency $\omega = 1$ can be regarded as a threshold value. In fact, referring to Fig.4 we can notice that frequencies bigger than 1 allow for the existence of ranges of the second gradient parameter corresponding to which we can detect an inverse behavior: the bigger amount of energy is reflected and cannot pass through the discontinuity surface. This means that for high frequencies the micro-structural inhomogeneity of the material starts playing a predominant role.

Considerations for the generalized internal roller are completely reversed with respect to those just made for the generalized internal hinge.

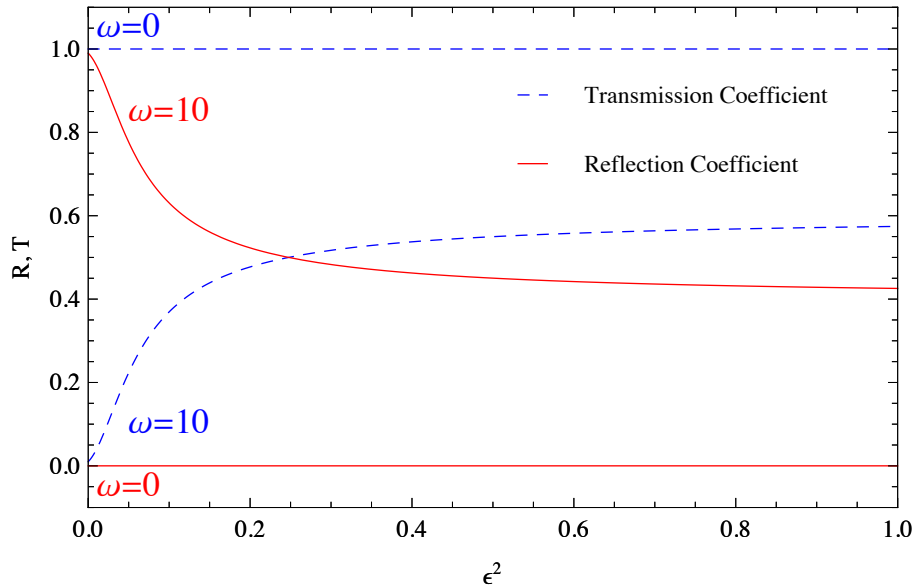


Figure 4: Reflection and transmission coefficients in presence of a generalized internal hinge for high frequencies. The plots for the generalized internal roller are completely specular: the blue dashed lines must be referred to the reflection coefficient, while the red lines must be referred to the transmission coefficient.

7 Conclusions

The presented results are a first step in the direction of the establishment of an experimental method for getting measurements of second gradient parameters in second gradient continua. We propose to use a discontinuity surface between two macroscopically homogeneous second gradient solids and the measurements of reflection and transmission coefficients at this interface as a method for measuring the bulk properties of considered continua. In the present paper we simply assume that the discontinuity surface is the only possible localization of displacement (and normal gradient of displacement) eventual jumps. More complicated discontinuity surfaces may be conceived carrying themselves mechanical properties and directly influencing transmission and reflection coefficients. Although the investigation of the behavior of such more general discontinuity surfaces is of importance, the simplest discontinuity we considered here seems the most suitable for getting estimates of bulk second gradient elastic moduli. Indeed, performing such a kind of experimental indirect measurements by using reflection and transmission of plane waves would undoubtedly be of great scientific and technological interest. In fact, the field of second gradient continuum theories, even if it is attracting much more interest in the last years, still receives some criticism due to the fact that no experimental measurements

are available in the literature. Measuring second gradient elastic moduli for a certain class of solids would then be useful as a starting point for further investigations. More complicated subsequent analyses should involve the study of reflection and transmission properties at structured interfaces between second gradient solids, at permeable and impermeable interfaces between different porous media in presence of Darcy-type fluid flow, interfaces between damaged and undamaged solids.

The results obtained in the last section of this paper show that also the boundary layer which may arise in the simplest second gradient solid greatly influence wave transmission and reflection.

8 References

- [1] Aifantis 2003. Update on a class of second gradient theories. *Mech. Materials* **35**, 259-280.
- [2] M.O.M. Carvalho & M. Zindeluk 2001. Active control of waves in a Timoshenko beam. *Int. J. Solids Struct.* **38**, 1749-1764
- [3] P. Casal 1961. La capillarité interne, *cahier du group francais de rhéologie, CNRS* **6**, 31-37.
- [4] P. Casal & H. Gouin 1985. Relation entre l'équation de l'énergie et l'équation du mouvement en théorie de Korteweg de la capillarité. *C.R. Acad. Sci. Paris* **300** II 7, 231-235.
- [5] E. Cosserat & F. Cosserat 1909. Sur la théorie des corps déformables. Herman, Paris, 1909.
- [6] P. G. de Gennes 1981. Some effects of long range forces on interfacial phenomena. *J. Physique Lettres* **42**, L-377, L-379
- [7] F. dell'Isola & P. Seppecher 1995. The relationship between edge contact forces, double force and interstitial working allowed by the principle of virtual power. *CRAS - Serie IIB: Mécanique, Physique, Chimie, Astronomie* **321**, 303-308
- [8] F. dell'Isola, H. Gouin, P. Seppecher 1995. Radius and Surface Tension of Microscopic Bubbles by Second Gradient Theory. *CRAS IIB Mechanics* **320**, 211-216
- [9] F. dell'Isola, H. Gouin, G. Rotoli 1996. Nucleation of Spherical Shell-Like Interfaces by Second Gradient Theory: Numerical Simulations. *Eur. J. Mech., B/Fluids* **15:4**, 545-568
- [10] F. dell'Isola & P. Seppecher 1997, Edge Contact Forces and Quasi-Balanced Power. *Meccanica* **32** (1997) 33-52
- [11] F. dell'Isola, A. Madeo, P. Seppecher 2009a. Boundary Conditions at Fluid-Permeable Interfaces in Porous Media: A Variational Approach. *Int. J. Solids Struct.* **46**, 3150-3164
- [12] F. dell'Isola, G. Sciarra, S. Vidoli 2009b. Generalized Hooke's law for isotropic second gradient materials, *Proc. R. Soc. A* **465**, 2177-2196
- [13] F. dell'Isola and P. Seppecher 2010. Commentary about the paper " Hypertractions and hyperstresses convey the same mechanical information Continuum

- Mech. Thermodyn 22:163176 ” by Prof. Podio Guidugli and Prof. Vianello and some related papers on higher gradient theories. hal-00495800
- [14] P. Germain 1973a. La méthode des puissances virtuelles en mécanique des milieux continus Première partie: Théorie du second gradient, *J. Mécanique* **12:2**, 235-274
- [15] P. Germain 1973b. The method of virtual power in continuum mechanics Part 2: Microstructure, *S.I.A.M. J. Appl. Math.* **25: 3**, 556-575
- [16] J.- L. Guyader 2006. Vibration in Continuous Media, ISTE Ltd, Chippenham
- [17] J. G. Harris 2004. Linear Elastic Waves, Cambridge University Press, Cambridge
- [18] A. Madeo, F. dell’Isola, N. Ianiro and G. Sciarra 2008. A Variational Deduction of Second Gradient Poroelasticity II: an Application to the Consolidation Problem. *J. Mech. Materials Struct.* **3:4**, 607625.
- [19] M. Ouisse, J.-L. Guyader 2003. Vibration Sensitive Behaviour of a connecting angle. Case of Coupled Beams and Plates, *J. Sound and Vibration* **267**, 809-850
- [20] G. Sciarra, F. dell’Isola, N. Ianiro and A. Madeo 2008. A Variational Deduction of Second Gradient Poroelasticity I: General Theory, *J. Mech. Materials Struct.* **3:3** (2008) 507-526.
- [21] R.A. Toupin 1962. Elastic materials with couple-stresses. *Arch. Rat. Mech. Anal.* **11**, 385-414.
- [22] R.A. Toupin 1964. Theories of elasticity with couple-stresses. *Arch. Rat. Mech. Anal.* **17**, 85-112.
- [23] N. Triantafyllidis, S. Bardenhagen 1996. The Influence of Scale Size on the Stability of Periodic Solids and the Role of Higher Order Gradient Continuum Models. *J. Mech. Phys. Solids* **44:11**, 1891-1928
- [24] Y. Yang, A. Misra 2010. Higher-Order Stress-Strain Theory for Damage Modeling Implemented in an Element-free Galerkin Formulation. *CMES* **1549:1**, 1-36